Organic Geochemistry 154 (2021) 104200

Contents lists available at ScienceDirect

Organic Geochemistry

journal homepage: www.elsevier.com/locate/orggeochem

Identifying marine and freshwater overprints on soil-derived branched GDGT temperature signals in Pliocene Mississippi and Amazon River fan sediments

Emily Dearing Crampton-Flood [a,1], Carolien M.H. van der Weijst [a], Guido van der Molen [a], Magali Bouquet [a], Yord Yedema [a], Timme H. Donders [b], Francesca Sangiorgi [a], Appy Sluijs [a], Jaap S. Sinninghe Damsté [a,c], Francien Peterse [a,*]

[a] Department of Earth Sciences, Faculty of Geosciences, Utrecht University, Vening Meinesz Building A, 3584 Utrecht, the Netherlands
[b] Department of Physical Geography, Faculty of Geosciences, Utrecht University, Vening Meinesz Building A, 3584 Utrecht, the Netherlands
[c] Department of Marine Microbiology and Biogeochemistry, and Utrecht University, NIOZ Royal Netherlands Institute for Sea Research, 17900 AB Den Burg, Texel, the Netherlands

ARTICLE INFO

Article history:
Received 17 September 2020
Received in revised form 9 February 2021
Accepted 10 February 2021
Available online 17 February 2021

Keywords:
BrGDGTs
Pliocene
Terrestrial temperature
Proxy limitations

ABSTRACT

The fractional abundance of branched glycerol dialkyl glycerol tetraether (brGDGT) membrane lipids in coastal marine sediments has been posited as a proxy for the reconstruction of terrestrial temperatures on the nearby land, based on the assumption that they are produced in soils and delivered to the marine realm by rivers following erosion. Here, we test the suitability of brGDGTs as a continental paleothermometer in Pliocene age sediments from the northern Gulf of Mexico (GoM; speculated Mississippi River input) and the Ceará Rise (speculated Amazon River input). Low branched to isoprenoid tetraether (BIT) index values of 0.00–0.13 and the near absence of pollen and long-chain plant waxes in the GoM sediments suggest that the Mississippi River did not have a strong influence on the delivery of terrestrial organic matter to the site during the Pliocene and soil input was limited. Indeed, the high weighted average of cyclopentane-containing tetramethylated brGDGTs (#rings$_{tetra}$) in the GoM sediments (0.50 ± 0.09) relative to that of modern soils from the Mississippi catchment (0.25 ± 0.16) indicates that the brGDGTs in the GoM sediments were mostly produced in situ in the marine realm, hampering reliable land temperature reconstruction using the global soil transfer function. In contrast, high BIT index values (0.46 ± 0.21) and low #rings$_{tetra}$ (0.25 ± 0.15) in sediments from the Ceará Rise suggest that these brGDGTs are primarily derived from soils. However, reconstructed temperatures were 11–18 °C lower than modern Amazon catchment temperatures. The relative abundance of 6-methylated brGDGTs (Isomerisation Ratio; IR) in the sediments is 0.82 ± 0.10, which resembles that of suspended particulate matter (SPM) in the modern Amazon River more than that of catchment soils (IR = 0.18 ± 0.18). This reveals that brGDGTs in the Ceará Rise sediments likely have a freshwater, riverine origin. Thus, the majority of the brGDGTs in both the GoM and Ceará Rise sediments are produced in situ, in the marine or river realms, which precludes application of the brGDGT paleothermometer. Our study shows that the sources of brGDGTs in coastal marine sediment archives must be critically evaluated prior to using the proxy for paleoclimate reconstruction.

1. Introduction

Branched glycerol dialkyl glycerol tetraethers (brGDGTs) are a compound class that forms the membrane lipid monolayer of bacteria occurring in soils and other environments (Sinninghe Damsté et al., 2000; Weijers et al., 2006). The brGDGTs are composed of two alkyl chains bound to two glycerol moieties by ether bonds and can vary in the number of methyl branches and cyclopentane moieties (Supplementary Fig. S1). Although the exact producer(s) of brGDGTs is unknown, their abundance in soils varies with that of Acidobacteria (Weijers et al., 2006, 2009, 2010), and low amounts of brGDGT Ia were identified in two species of Acidobacteria, a bacterial phylum of which many members produce a presumed building block of brGDGTs, *iso*-diabolic acid (Sinninghe Damsté et al., 2011, 2018). An empirical study on brGDGT occur-

* Corresponding author.
E-mail address: f.peterse@uu.nl (F. Peterse).
[1] Present address: NLO Patents and Trademarks, Bennekomsweg 43, 6717 LL Ede, the Netherlands.

https://doi.org/10.1016/j.orggeochem.2021.104200
0146-6380/

rence in soils and peats worldwide showed that the degree of methylation of brGDGTs relates to mean annual air temperature (MAAT) and soil pH, whereas the degree of cyclisation is linked to soil pH (Weijers et al., 2007a). Initially, a combination of these two relationships was used to quantitatively reconstruct MAAT. After the identification of isomers of the penta- and hexamethylated brGDGTs, which are distinguished by the varying position of the methyl group present on either the 5- or 6-position of the alkyl chain (De Jonge et al., 2013; Supplementary Fig. S1), and improvement in chromatographic separation used to analyse brGDGTs (Hopmans et al., 2016), the degree of methylation of 5-methyl brGDGTs was found to be dominantly temperature-controlled leading to a pH-independent transfer function (De Jonge et al., 2014a).

Upon mobilization, fluvial transport and discharge, soil brGDGTs can be archived in coastal marine sediments, where they can be used to determine the relative input of river-transported soil organic matter (OM) to marine sediments. This input is quantified by the Branched and Isoprenoid Tetraether (BIT) index (Hopmans et al., 2004), in which the abundance of soil-derived brGDGTs is taken relative to that of the isoprenoidal GDGT (isoGDGT) crenarchaeol, produced by marine Thaumarchaeota (Sinninghe Damsté et al., 2002). Hence, a high BIT index is indicative of substantial input of soil organic matter to the site, providing that sources of brGDGTs are 100% soil-derived. Thus, a high BIT index calculated in a marine sedimentary archive usually indicates the suitability of the site for the reconstruction of past air temperatures of the nearby continent. Indeed, analysis of brGDGTs stored in Congo River fan sediments resulted in a temperature record for tropical east Africa over the last deglaciation (Weijers et al., 2007b). Since then, MAAT records have been generated for a variety of marine sites including high latitudes (Weijers et al., 2007c; Sangiorgi et al., 2018), and go as far back in time as the Cretaceous (Kemp et al., 2014; Super et al., 2018), indicating excellent preservation of these molecular fossils.

However, caution must be taken due to potential in situ production of brGDGTs in marine environments. This has been documented in surface sediments in Svalbard (Peterse et al., 2009), the Brazilian Margin (Zell et al., 2014), the Kara Sea (De Jonge et al., 2015), Portuguese margin (Warden et al., 2016), Baltic Sea (Warden et al., 2018), the Berau Delta (Indonesia; Sinninghe Damsté, 2016), East China Sea (Zhu et al., 2011), and the Brazilian margin (Ceccopieri et al., 2019). These in situ produced brGDGTs can be recognized by a high degree of cyclisation of the tetramethylated suite of brGDGTs, expressed as the $\#rings_{tetra}$ (Sinninghe Damsté, 2016). The increased cyclisation is most likely a response to the relatively more alkaline environment in the ocean compared to soils (Sinninghe Damsté, 2016), of which only 14% in the global soil and peat dataset have a pH > 8 (De Jonge et al., 2014a; Naafs et al., 2017; Dearing Crampton-Flood et al., 2020). A value of $\#rings_{tetra} > 0.7$ is used as a cut-off to indicate unequivocal marine in situ production based on the fact that $\#rings_{tetra}$ is always < 0.7 in the global soil calibration set. This index subsequently formed the base for an end-member method that enabled disentangling marine and soil-derived brGDGTs in the Pliocene section of the Hank borehole from the North Sea, and to correct the continental air temperature record for the overprint of marine in situ produced brGDGTs (Dearing Crampton-Flood et al., 2018). This successful test case encourages the wider application of the brGDGT paleothermometer to coastal marine sediments to generate more Pliocene terrestrial temperature records.

Here, we aim to reconstruct terrestrial temperatures for two of the world's largest river catchments using brGDGTs preserved in Pliocene sediments relatively near the Mississippi (Ocean Drilling Program, ODP Site 625) and Amazon River outflows (ODP Site 925). We specifically target the mid-Piacenzian Warm Period (mPWP; 3264–3025 ka), as its warmer (ΔT = +2–3 °C; Haywood et al., 2020) climate is often considered as an analogue for near-future climate (Masson-Delmotte et al., 2013; Burke et al., 2018). The Mississippi and Amazon have a modern annual sediment discharge of 6.2×10^{11} kg (Coleman, 1988) and $7–8 \times 10^{11}$ kg (Martinez et al., 2009), respectively. Previous studies have indicated that both rivers were active during the Pliocene (Coleman, 1988; Figueiredo et al., 2009). The influence of the Pliocene Mississippi River on sediments on the continental shelf and slope of the Northern Gulf of Mexico (GoM) is supported by the presence of pollen in Miocene to Pleistocene sediments from offshore Louisiana (Elsik, 1969). We improve stratigraphic constraints at ODP Site 625 by generating a record of benthic foraminifer oxygen isotope ratios ($\delta^{18}O$), which we correlate to the dated stack of Lisiecki and Raymo (2005). A 30 Myr BIT index record for ODP Site 925, which has a highly resolved stratigraphy (Wilkens et al., 2017) reveals substantial input of fluvially discharged soil material during the Pliocene (van Soelen et al., 2017). This should support the application of the brGDGT paleothermometer at both sites.

2. Materials and methods

2.1. Study sites

2.1.1. Mississippi River delta

In the modern GoM, the surface Loop Current transports relatively warm and salty water through the Yucatán Channel from the Caribbean Sea, eventually exiting through the Florida Strait (Fig. 1). The extension of the Loop Current into the basin depends on the Intertropical Convergence Zone (ITCZ), which migrates seasonally (Nürnberg et al., 2008).

ODP Site 625 (28°49.9′N, 87°09.6′W; water depth 889 m) is located on the west Florida continental slope in the North Eastern Gulf of Mexico, approximately 200 km southeast from the current mouth of the Mississippi River (Fig. 1A). Modern influence of the Mississippi River discharge to the site is determined by lower sea surface salinity values compared to the western GoM (Nürnberg et al., 2008). We sampled the interval at 129–165 m below sea floor (mbsf) of Hole B, which consists of marly nannofossil ooze and calcareous mud (Rabinowitz et al., 1985). Based on the preliminary biostratigraphic age model of Joyce et al. (1990), the chosen interval should cover the period from ~2.5–4.0 Ma. The interval was further dated using benthic $\delta^{18}O$ stratigraphy.

2.1.2. Amazon River delta

ODP Site 925 (4°12.248′N, 43°29.349′W; water depth 3040 m) is located on the Ceará Rise, approximately 800 km northeast from the current mouth of the Amazon River (Fig. 1B). In modern and near-recent times, Site 925 receives a large amount of terrestrial material from the Amazon River, evidenced by organic and inorganic proxies (van Soelen et al., 2017). The relative positions of the Ceará Rise and South America did not change significantly over the Cenozoic (Curry et al., 1995). However, the discharge of the Amazon River is postulated to have intensified after its transcontinental connection to the Andes at ~9 Ma (van Soelen et al., 2017; Lammertsma et al., 2018).

We studied the 75–133 mbsf interval of Hole B, which consists of nannofossil ooze (Curry et al., 1995), and spans 2.3–5.3 Ma according to the orbitally tuned age model of Wilkens et al. (2017). Fourteen sediment samples within this interval were selected for GDGT analysis and complemented with nine additional data points previously reported by van Soelen et al. (2017).

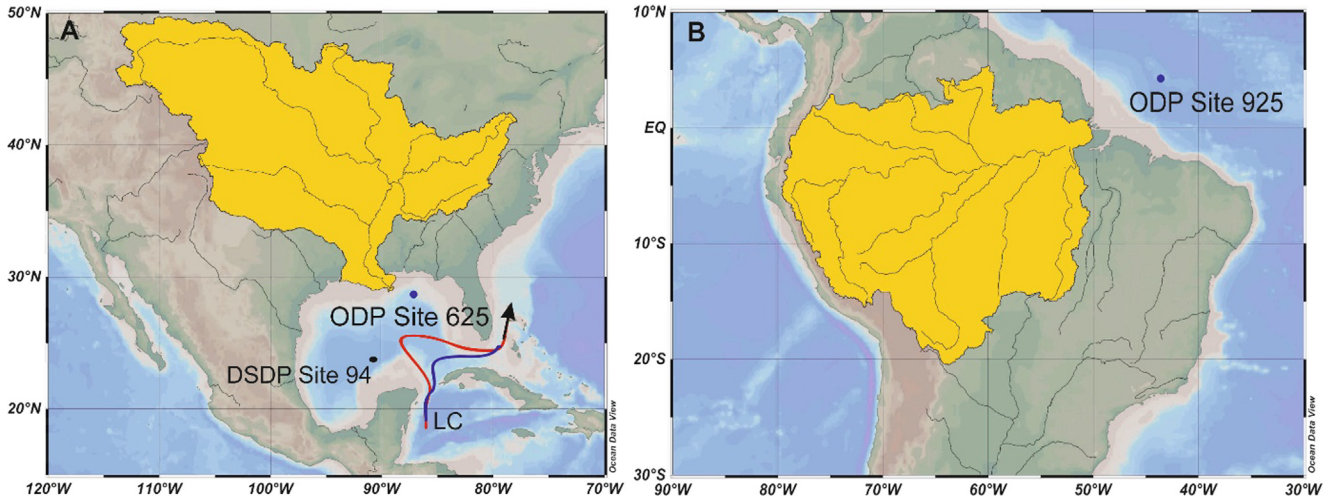

Fig. 1. Locations of: (A) ODP Site 625 and DSDP Site 94 in the Gulf of Mexico, and (B) ODP Site 925 on the Ceará Rise. The modern watersheds of the (A) Mississippi and (B) Amazon Rivers are shaded in yellow. The position of the Loop Current (LC) in the Gulf of Mexico during austral summer (red) and fall/winter (blue) is shown. (For interpretation of the references to colour in this figure legend, the reader is referred to the web version of this article.)

2.2. Site 625 oxygen isotope analysis and stratigraphy

Site 625 was previously roughly dated by obliquity tuning of planktonic foraminiferal $\delta^{18}O$ (Joyce et al., 1990). The early Pleistocene (90–120 mbsf) was later revisited using benthic $\delta^{18}O$ stratigraphy by Shakun et al. (2016), who arrived at ages ~100–200 kyr older than Joyce et al. (1990). Here, we revisit the late Pliocene interval between ~130–160 mbsf using benthic $\delta^{18}O$ stratigraphy, which corresponds to 2570–3460 ka on the age model of Joyce et al. (1990). However, in accordance with the Pleistocene interval (Shakun et al., 2016), we expect to arrive at somewhat older ages.

Samples were taken at ~15 cm intervals from cores 625B-16H to 625B-19H, freeze-dried, wet sieved, and oven dried overnight at a low temperature. From each sample, we typically picked four moderately to well-preserved specimens of *Cibicides wuellerstorfi* from the > 250 μm size fraction. Isotope analyses were performed at the Faculty of Geosciences, Utrecht. Samples between 129.98 and 149.03 mbsf were analysed with a Thermo-Finnigan Kiel IV automated preparation system coupled to a Thermo-Finnigan MAT 253 Plus mass spectrometer. Samples between 149.18 and 159.1 mbsf were analysed with a Thermo Finnigan GasBench-II carbonate preparation device coupled to a Thermo Finnigan Delta-V mass spectrometer. Analytical precision was 0.03‰ for $\delta^{18}O$ and 0.05‰ for $\delta^{13}C$ on the GasBench system. The Kiel setup was new at the time and incidentally less precise as a consequence, with a reproducibility of 0.23‰ for $\delta^{18}O$ and 0.11‰ for $\delta^{13}C$. The data were calibrated to the international standard (VPDB) and the $\delta^{18}O$ record was corrected with + 0.64‰ following Shackleton (1974).

Cores 625B-18H and 625B-19H overlap by 1.73 m on the mbsf depth scale. Because the Pliocene was only recovered from Hole B, a splice is not available. We assume that this overlap is related to sediment expansion and applied a correction of + 2.0 m to samples from cores 625B-19H and 625B-20H. We report the data on a revised mbsf (rmbsf) scale. The age model was constructed by visual correlation of the benthic $\delta^{18}O$ record on the rmbsf scale to the LR04 benthic isotope stack (Fig. 2; Lisiecki and Raymo, 2005).

2.3. Lipid biomarker extraction and analysis

Sediments from ODP Site 625 (n = 177) and Site 925 (n = 14) cores were freeze dried and powdered prior to extraction (3 ×) using a dichloromethane (DCM):methanol (9:1, v/v) solvent mixture in an accelerated solvent extractor (ASE 350, Dionex). The ASE extraction method consisted of a 5 min extraction at 100 °C and 7.6 × 10^6 Pa. The total lipid extract (TLE) was dried under nitrogen and separated into apolar, ketone, and polar fractions using activated Al_2O_3 in a small column using hexane:DCM (9:1, v/v), hexane:DCM (1:1, v/v) and DCM:methanol (1:1, v/v) as eluents, respectively. Polar fractions were prepared for GDGT analysis first by the addition of a known amount of an internal standard (C_{46} glycerol trialkyl glycerol tetraether, GTGT; Huguet et al., 2006), then by dissolving the (dry) fraction in hexane:isopropanol (99:1, v/v) prior to filtering using a 0.45 μm PTFE filter.

Reanalysed suspended particulate matter (SPM) samples from Zell et al. (2013a) and samples from ODP Site 925 were analysed for GDGTs at the Royal Netherlands Institute for Sea Research (NIOZ). All samples from ODP Site 625 were measured at Utrecht University (UU). At both institutes, brGDGTs were analysed following the method described by Hopmans et al. (2016). In short, an Agilent 1260 Infinity ultra high performance liquid chromatography (UHPLC) instrument coupled to an Agilent 6130 single quadrupole mass detector was used for analysis. Two silica Waters Acquity UPLC BEH Hilic columns (1.7 μm, 2.1 mm × 150 mm) at 30 °C and a guard column was used for chromatographic separation. The solvent program, for which hexane (A) and hexane:isopropanol (9:1, v/v) (B) were used, followed isocratic elution at a flow rate of 0.2 ml/min with 82% A and 18% B for 25 min, followed by a linear gradient to 70% A and 30% B for 25 min. 10 μL of sample was injected. Ionisation of GDGTs was achieved using atmospheric pressure chemical ionisation (APCI) using the following source conditions: gas temperature 200 °C, vaporizer temperature 400 °C, capillary voltage 3500 V, nebulizer pressure 25 psi, drying gas (N_2) flow 6 L/min, corona current 5.0 μA. Selected ion monitoring (SIM) was used to identify the GDGTs using their $[M-H]^+$ ions: *m/z* 1292, 1050, 1048, 1046, 1036, 1034, 1032, 1022, 1020, 1018. The internal GTGT standard was identified using *m/z* 744. GDGTs were integrated using Chemstation software B.04.02.

A selection of apolar fractions from Sites 625 and 925 were analysed for plant leaf epicuticular waxes using gas chromatography with flame ionization detection (GC-FID). Samples were desulfurized and analysed using manual injection (1 μL) on a Hewlett Packard 6890 series GC system equipped with a 0.53 mm precolumn and CP-Sil 5 fused silica capillary column (25 m × 0.32 m m; film thickness 0.12 μm). The samples were initially held at

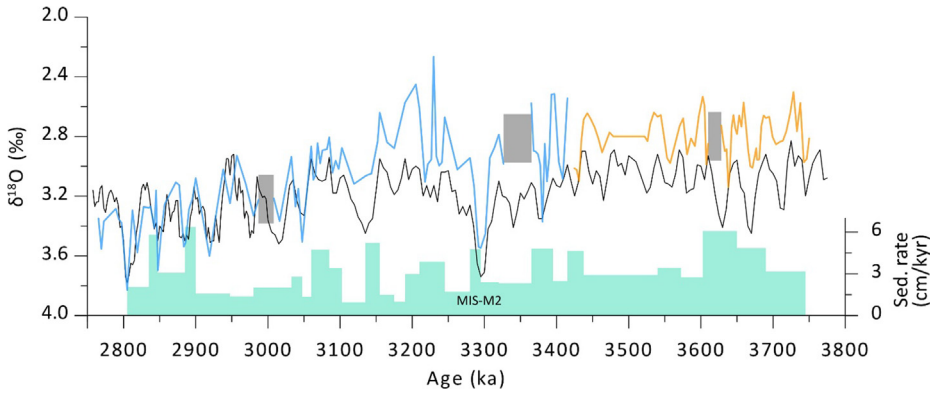

Fig. 2. Top: Site 625 benthic $\delta^{18}O$ record (blue: Kiel method; orange: Gasbench method) and the LR04 tuning target (Lisiecki and Raymo, 2005; black). Bottom: sedimentation rates (green) calculated with the rmbsf depth scale. Grey shaded intervals indicate core gaps. (For interpretation of the references to colour in this figure legend, the reader is referred to the web version of this article.)

70 °C (1 min), ramped to 130 °C (20 °C min^{-1}), ramped to 320 °C (4 °C min^{-1}), and held for 25 min.

2.4. GDGT proxy calculations

The MBT′5Me index was calculated using the following equation (De Jonge et al., 2014a):

$$MBT'5Me = \frac{[Ia] + [Ib] + [Ic]}{[Ia] + [Ib] + [Ic] + [IIa] + [IIb] + [IIc] + [IIIa]} \quad (1)$$

Mean annual air temperatures were calculated using the most recent soil and peat calibration based on Bayesian methodology (Dearing Crampton-Flood et al., 2020) and brGDGT data from De Jonge et al. (2014a) and Naafs et al. (2017), with a prior mean of 15 °C and prior standard deviation of 15.

BIT indices were calculated according to the following equation, adjusted to include both 5- and 6-methyl GDGTs (Hopmans et al., 2004);

$$BIT = \frac{[Ia] + [IIa] + [IIa'] + [IIIa] + [IIIa']}{Cren + [Ia] + [IIa] + [IIa'] + [IIIa] + [IIIa']} \quad (2)$$

where Cren refers to crenarchaeol.

The isomer ratio (IR), which expresses the relative proportion of 6-methyl brGDGTs over the total sum (De Jonge et al., 2015), was calculated as follows:

$$IR = \frac{[IIa'] + [IIb'] + [IIc'] + [IIIa'] + [IIIb'] + [IIIc']}{[IIa'] + [IIb'] + [IIc'] + [IIIa'] + [IIIb'] + [IIIc'] + [IIa] + [IIb] + [IIc] + [IIIa] + [IIIb] + [IIIc]} \quad (3)$$

Numbers refer to structures of brGDGTs in Supplementary Fig. S1.

The number of rings of tetramethylated brGDGTs was calculated according to the following (Sinninghe Damsté, 2016):

$$\#rings_{tetra} = \frac{([Ib] + 2 \times [Ic])}{([Ia] + [Ib] + [Ic])} \quad (4)$$

3. Results and discussion

3.1. Mississippi River basin

3.1.1. ODP Site 625 age model

The benthic $\delta^{18}O$ record is plotted in Fig. 2. The Marine Isotope State (MIS)-M2 glacial clearly stands out between 144.40 and 144.83 rmbsf (Supplementary Table S1) and was used as the initial tie point with the LR04 stack. There is generally good coherence between the Site 625 isotope stack and LR04, particularly in the younger part of the record. However, the interval prior to M2 does not display particularly outstanding isotope events. In combination with several intervals with unrecovered sediment, such as a 1.2 m gap around ~150 rmbsf in section 625B-18H-4, there is considerable uncertainty in the tuning, and alternative correlations to the LR04 stack could be made. The sedimentation rate varies around an average of 3.1 cm/kyr on average, similar to the Pleistocene interval (Shakun et al., 2016).

In the younger part of our studied interval, the benthic $\delta^{18}O$ values are similar to the LR04 stack (Lisiecki and Raymo, 2005), consistent with the Pleistocene interval of Shakun et al. (2016). However, around 3100–3200 ka, the Site 625 oxygen isotope record shifts ($\Delta^{18}O$ = 0.8‰) towards lower values. This shift is not related to the switch in experimental setup from Kiel to Gasbench at ~3431–3434 ka. Because the study site is relatively shallow (889 m), it is more susceptible to regional oceanographic changes than the majority of the deep ocean records from which LR04 was constructed. The $\delta^{18}O$ shift may instead be explained by local changes in circulation, temperature and/or salinity.

3.1.2. Temperature reconstruction for the Mississippi River basin

GDGTs are present throughout the studied interval of Site 625 sediments, where the isoGDGT crenarchaeol is always more abundant than brGDGTs. Of the brGDGTs, the most abundant compound is Ia (average fractional abundance 28.6 ± 4.5%), followed by Ib (10.0 ± 1.1%). BrGDGTs IIIc and IIIc′ were below the detection limit in all but two sedimentary horizons. The BIT record (Fig. 3B) indicates that the pool of GDGTs at Site 625 is dominated by marine OM throughout most of the Pliocene interval since average BIT values (i.e., 0.04 ± 0.02) are low (Hopmans et al., 2004; Schouten et al., 2013 and References therein). However, variations in BIT can be driven by changes in the abundance of brGDGTs and of crenarchaeol. As a result, the BIT can be low when there is high crenarchaeol production due to increased nutrient input from land, even though the absolute amount of brGDGTs may be high. For example, a dominance of marine OM manifested by low BIT values (< 0.2) was also observed at the Hank borehole located in the Pliocene North Sea (Dearing Crampton-Flood et al., 2018). However, the presence of other indicators for terrestrial input, such as pollen (bisaccate and non-bisaccate), confirmed that the Hank site

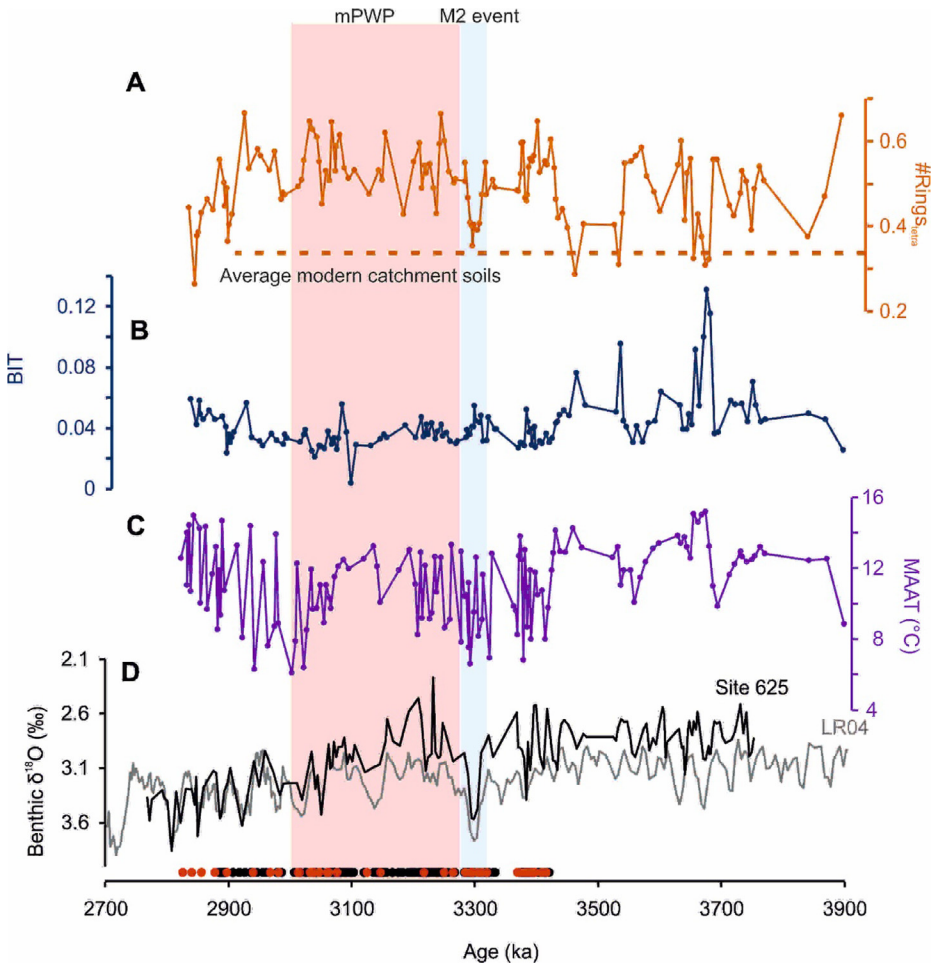

Fig. 3. Proxy records for the Pliocene ODP Site 625 sediments in the Gulf of Mexico. (A) #rings$_{tetra}$, (B) BIT, (C) MAAT, and (D) ODP 625 (black) and LR04 benthic $\delta^{18}O$ records (grey) plotted against age. Samples analysed for pollen (red circles) and *n*-alkane composition (black circles) are shown on top of the age axis. (For interpretation of the references to colour in this figure legend, the reader is referred to the web version of this article.)

received substantial terrestrial input, validating the reconstruction of temperatures from (terrestrially derived) brGDGTs.

In contrast, plant leaf wax biomarkers and pollen (not shown) are virtually absent in Site 625 sediments, confirming the BIT results that indicate that the input of terrestrial material was minimal at this site. The distance of Site 625 to the mouth of the Mississippi may have played a role in the low BIT indices, as the concentration of brGDGTs in modern continental margin sediments rapidly decreases with increasing distance from the coast at the Tagus River outflow, the East Siberian Arctic Shelf, and the Berau delta in Indonesia (Zell et al., 2015; Sparkes et al., 2015; Sinninghe Damsté, 2016). In addition, a higher sea level (~13–25 m) during the mid and late Pliocene documented by models (e.g., de Boer et al., 2017) and "backstripped" estimates (Grant et al., 2019) would have positioned the Mississippi River mouth relatively further away from Site 625, contributing to a low abundance of terrestrially derived brGDGTs at the more distal site.

Interestingly, a previous study on a sediment core from the central GoM (DSDP Site 94; Fig. 1A) reported carbon and hydrogen isotopic compositions of terrestrial leaf waxes over the last 35 Myr (Tipple and Pagani, 2010), thus indicating that terrestrial material did reach the central basin during the Pliocene. DSDP Site 94 is located 300 km further away from the mouth of the Mississippi River than Site 625, hence the lack of plant waxes at Site 625 is startling since terrestrial material should pass by Site 625 before reaching the central GoM. This suggests that in contrast to a higher sea level, the near absence of terrestrial leaf waxes and pollen at Site 625 is more likely a result of a changed direction of the Mississippi River outflow during the Pliocene. Sedimentological evidence implies that the axis of the Mississippi outflow pointed more towards the west during the Miocene/Pliocene than at present, due to the location of the Pliocene Mississippi GoM depocenters in the North Western Gulf Margin near the Texas and Louisiana border, where the shelf edge prograded most rapidly (Woodbury et al., 1974; Galloway et al., 2011; Bentley et al., 2016). Other sedimentological and palynological evidence indicates this was also the case during MIS6, where variations in dinocysts sensitive to changing salinity were thought to reflect a change in direction of the Loop Current during warmer/cooler periods (Fig. 1A; Tripsanas et al., 2007; Limoges et al., 2014). However, pollen assemblages in sediments from offshore Louisiana still suggest a limited influence of the Mississippi River to Site 625 during the Pliocene (Elsik, 1969). In any case, abundant terrestrial palynomorphs in Site 625 sediments from the late Pleistocene to the Holocene indicate that the Mississippi outflow was similar to its present position at that time (Limoges et al., 2014). This suggests that a change in the location of the Mississippi outflow, perhaps coupled to the strength and position of the Loop Current, may at least partly be responsible for the low abundance of terrestrial material in the Pliocene Site 625 sediments. In any case, the presence of brGDGTs in the sediment core provides the minimum requirement for the attempted application of the brGDGT pale-

othermometer in these sediments. Nevertheless, the limited evidence for terrestrial influence at this site indicates that a source assessment of the brGDGTs is needed to validate the reliability of reconstructed MAATs.

The source(s) of the brGDGTs that are present in Site 625 sediments can be evaluated by comparing the relative amounts of the tetra-, penta-, and hexamethylated brGDGTs with that of global soils in a ternary plot (cf. Sinninghe Damsté, 2016). The GoM sediments clearly plot offset from the typical soil pattern (Fig. 4), suggesting that a substantial proportion of brGDGTs at Site 625 has a non-soil origin. Indeed, the #rings$_{tetra}$, which can be used as a measure to identify in situ brGDGT production in coastal marine sediments (e.g., Sinninghe Damsté, 2016), in the GoM sediments ranges from 0.26 to 0.67 (Fig. 3A). The average of 0.50 ± 0.08 is much higher than that in global soils (0.21 ± 0.19) and that of the soils in the modern catchment of the Mississippi, which is 0.34 ± 0.22 (n = 7; De Jonge et al., 2014a), indicating that at least part of the brGDGTs at this site are produced in situ. The #rings$_{tetra}$ record varies over time and shows a few clear minima and a general trend toward lower #rings$_{tetra}$ values after 3.0 Ma (Fig. 3A). One of the minima in the #rings$_{tetra}$ record at 3.65 Ma coincides with a minor increase of the BIT index from 0.02 to 0.12 and relatively warmer MAATs (Fig. 3). This trend suggests either: (i) an increased input of soil-derived brGDGTs, (ii) a reduced marine in situ produced brGDGT overprint, or (iii) a change in marine in situ brGDGT distributions. The drivers of this variability remain unclear, but may be related to the direction of the Mississippi outflow or changing currents driving salinity/temperature gradients in the GoM, or a combination of the two.

As a likely result of marine brGDGT production, MAATs generated by the Bayesian temperature calibration and the MBT'5Me index (Dearing Crampton-Flood et al., 2020) exhibit neither a clear trend with time, nor a change to a cooler climate state in the latest Pliocene as seen in benthic isotope records (Lisiecki and Raymo, 2005). Moreover, the brGDGT-based MAATs (5.8–15.2 °C; Fig. 3C) generally underestimate the expected MAATs based on the current measured MAAT of 18–20 °C in the lower Mississippi catchment (Harris et al., 2014) and conflict with the general idea that global (and terrestrial) temperatures were 2–3 °C higher during the Pliocene (Haywood et al., 2016). Substantial brGDGT contributions from the upper catchment, where MAAT is lower, are considered unlikely based on studies from the modern Danube and Yangtze Rivers where brGDGT signals at the river mouth represented the lower catchment rather than an integration of the entire catchment (Li et al., 2015; Freymond et al., 2017). Notably, MAATs are also underestimated during periods with relatively low #rings$_{tetra}$ and higher BIT index values indicating a larger contribution of soil-derived brGDGTs to the site. Taken together, the absence of terrestrial biomarkers (e.g., leaf waxes) and pollen throughout this interval, in combination with overall low BIT index and high #rings$_{tetra}$ values indicates that the terrestrial input (including soil-derived brGDGTs) is too low to correct for the marine overprint on the soil-brGDGT signal with reasonable confidence (cf. Dearing Crampton-Flood et al., 2018). This makes it impossible to obtain a quantitative temperature record for Southern North America during the Pliocene based on brGDGT distributions in the sediments of ODP Site 625.

3.2. Temperature reconstruction for the Amazon River basin

BrGDGTs are present in all analysed sediments of ODP Site 925 (Ceará Rise) throughout the studied interval of ~5.3–2.3 Ma. In general, the most abundant brGDGT is Ia (44.0 ± 12.2%), followed by the 6-methylated brGDGTs IIa′ (9.7 ± 2.4%) and IIb′ (9.0 ± 5.8%). In contrast, the least abundant brGDGTs, IIIc, IIc, and IIIb, are all 5-methylated isomers. Considering the depth of the Site 925 (> 3000 m) and its distance from the Amazon River mouth (~800 km), an investigation of the brGDGT sources is required to assess the suitability of this site for MAAT reconstruction.

The Ceará Rise sediments generally have high BIT index values, ranging from 0.40 to 0.83 (average 0.58 ± 0.11; Fig. 5C), indicating a dominance of brGDGTs over crenarchaeol, typically interpreted to be indicative of a high terrestrial input (Hopmans et al., 2004). This interpretation is supported by the presence of higher plant leaf waxes synonymous of a vascular plant source (not shown). In addition, the #rings$_{tetra}$ ranges from 0.12 to 0.59 (Fig. 5B), which is well below the threshold value of 0.8 that identifies an in situ marine sedimentary source of brGDGTs (cf. Sinninghe Damsté, 2016), especially in sediments < 3.6 Ma. Comparison of the average #rings$_{tetra}$ in this record with the average from soils in the modern Amazon catchment, which is 0.10 ± 0.10 (n = 39; De Jonge et al., 2014a; Kirkels et al., 2020), indicates that the majority of the brGDGTs in the Amazon fan sediments presumably has a soil origin. Moreover, van Soelen et al. (2017) showed that after 4.5 Ma, the sedimentation of mineral and organic terrigenous material at Site 925 increases considerably due to Andean uplift. Similarly, Lammertsma et al. (2018) identified an increase in terrestrial input in a marine record from the Amazon fan after the (early) Pliocene. Given the encouraging values of the BIT and #rings$_{tetra}$ indices, the reconstruction of a temperature record appears viable at Site 925.

Reconstructed MAAT using MBT'5Me (De Jonge et al., 2014a) and the recent Bayesian soil calibration (Dearing Crampton-Flood et al., 2020) in the Ceará Rise sediments ranges from 9.9 °C to 25.9 °C (Fig. 5D). The variability in the MAAT record (5–15 °C) is remarkable given the supposedly equable climate during the Pliocene, especially in the subtropics (Herbert et al., 2010). Comparison with the modern-day MAAT of the Amazon River catchment (25–30 °C; Harris et al., 2014) shows that the brGDGT-based temperatures for the Pliocene are lower than today by ~5–20 °C, and thus most likely underestimate Pliocene temperatures, which are assumed to be > 2 °C than present (Haywood et al., 2016).

The Ceará Rise sediments plot offset from the global soils in the ternary plot of tetramethylated, pentamethylated, and hexamethylated brGDGTs (Fig. 4), implying that a proportion of the brGDGTs in Site 925 sediments is derived from other sources than soils. The pattern of the Ceará Rise sediments in the triplot is more widely distributed than that of other marine sediments, which tend to cluster together (Fig. 4). The distinct position of Site 925 in Fig. 4 may thus suggest a contribution of yet another source of brGDGTs than those produced in soils or the coastal marine environment to Site 925 Pliocene sediments.

A number of studies have indicated that brGDGTs can also be produced within rivers (Kim et al., 2012; Zhang et al., 2012; Zell et al., 2013a,b; Warden et al., 2016). In particular, the presence of brGDGTs with phospho- and glyco-headgroups still attached in SPM from the Amazon River provides strong evidence for brGDGT production within the river (Zell et al., 2013a), as these headgroups are presumed to be quickly lost upon cell death (White et al., 1979; Harvey et al., 1986). Furthermore, in situ production within the river was also used to explain offsets in brGDGT signals between soils and SPM from the Lower Amazon (Zell et al., 2013a; Moreira et al., 2014). Increased influence of in situ produced SPM-brGDGTs was observed in the rising water season that takes place from January to February (Zell et al., 2013b). Similarly, offsets between brGDGT signals in SPM and soils in the Pearl (Zhang et al., 2012), Yangtze (Yang et al., 2013), and the Yenisei Rivers (De Jonge et al., 2014b), as well as on a smaller scale in the Carminowe Creek catchment (Guo et al., 2020), were also attributed to an overprint by in situ produced brGDGTs. In the latter systems, brGDGTs in the river were characterized by a relatively high proportion of 6-methylated isomers. Interestingly, the penta- and hexamethylated brGDGTs in Site 925 sediments are also dominated by 6-

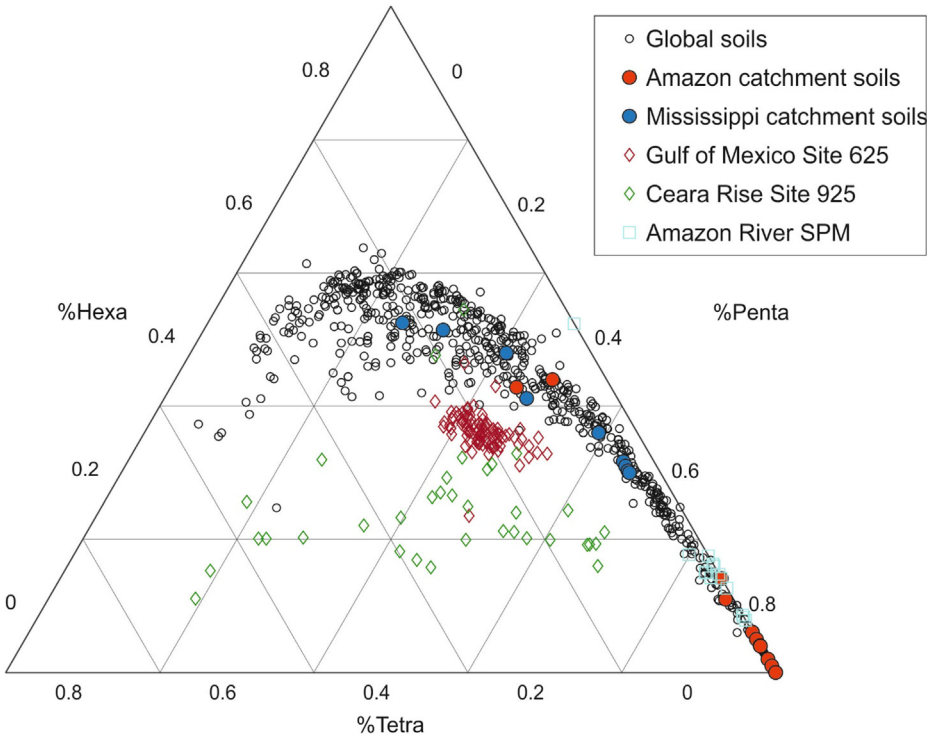

Fig. 4. Ternary diagram showing fractional abundances of the tetramethylated, pentamethylated, and hexamethylated brGDGTs for global soils and peats (black circles, De Jonge et al., 2014a; Naafs et al., 2017; Dearing Crampton-Flood et al., 2020), Pliocene Gulf of Mexico sediments (red diamonds), Amazon Fan sediments (green diamonds, this study and van Soelen et al., 2017), and Amazon River suspended particulate matter (blue squares, Zell et al., 2013a; Kirkels et al., 2020). Mississippi (blue) and Amazon (red) catchment soils are highlighted. (For interpretation of the references to colour in this figure legend, the reader is referred to the web version of this article.)

methylated brGDGTs. Quantifying their contribution using the isomerisation ratio (IR), results in IR values for Site 925 that are consistently high (0.79 ± 0.12) throughout the record (Fig. 5), except for a few lower values of ca. 0.5 at ~5 Ma and 4.3 Ma, although these shifts are based on one data point each.

In soils, the IR is positively correlated with pH (De Jonge et al., 2014b; Ding et al., 2015; Yang et al., 2015). Soils in the Amazon catchment are generally characterized by a low soil pH (Moreira and Fageria, 2009). This is reflected in low IR values (0.18 ± 0.18, n = 39; Fig. 6) for Amazon catchment soils included in the global brGDGT dataset (n = 13; De Jonge et al., 2014a) and the Madre de Dios River, an upper tributary of the Amazon River in South Eastern Peru (n = 26; Kirkels et al., 2020). The large difference in IR between catchment soils and Ceará Rise sediments (Fig. 6) could thus be caused by a contribution of brGDGTs produced in the Amazon River. Re-analysis of the SPM samples from Zell et al. (2013a) using the improved HPLC method (Hopmans et al., 2016) shows that the IR signature of SPM in the modern lower Amazon River is 0.38 ± 0.08 (Fig. 6), which is indeed higher than that of the soils. Similarly, brGDGTs in SPM from the Madre de Dios have an IR of 0.43 ± 0.14 (Kirkels et al., 2020; Fig. 6). Kirkels et al. (2020) also observed an increase in IR with decreasing altitude toward the Madre de Dios lowland area, which they attributed to enhanced riverine brGDGT production in areas with relatively lower turbidity and flow velocity. In particular, the SPM collected during the dry season in the Upper Amazon has a high IR (0.56 ± 0.10; Fig. 6), probably as a result of the decreased turbidity of the river water in the dry season, which may promote increased production of heterotrophic brGDGT-producing bacteria (Kirkels et al., 2020).

The absolute IR values in Site 925 sediments are higher than the modern river environment (Fig. 6), indicating that riverine brGDGT production in the Pliocene Amazon River may have been enhanced compared to present, either through a lower turbidity system present in the lowlands, or a drier climate that would have decreased soil and riverbank erosion and subsequently the sediment load in the river. In a modelling experiment using late Pliocene soils from a global dataset, Pound et al. (2014) determined a decrease in mean annual precipitation (MAP) of 30 mm month^{-1} over the Amazon region based on vegetation records, coinciding with a decrease in soil moisture. This data could lend credence to the hypothesis of a decreased sediment load in the Pliocene Amazon as the driver for high IR values. Alternatively, the offset between the IR values in Pliocene sediments compared to modern SPM riverine values may be attributed to brGDGTs produced in the deep marine environment. Recent studies investigating the brGDGT distributions in sediments from deep marine trenches (1.6–11 km), which hardly receive any terrestrial organic matter contribution, show a clearly distinct brGDGT distribution from other shallower marine sediments, with relatively higher IR and lower #rings$_{tetra}$ values (Xiao et al., 2020; Xu et al., 2020). Due to the depth (~3 km) of Site 925, a further contribution from deeper-dwelling brGDGT-producing organisms to the brGDGT distribution at the site cannot be discounted, but is unlikely to contribute a major fraction due to the relatively higher BIT, depleted $\delta^{13}C_{org}$ (van Soelen et al., 2017), and presence of plant leaf waxes in Site 925 sediments. Thus, we consider the bulk of brGDGTs in Pliocene sediments at Site 925 to be derived from the Amazon River.

The generally high IR signature of the Ceará Rise sediments (Fig. 6) most probably indicates a substantial riverine brGDGT overprint that disqualifies this site for the creation of an absolute MAAT record for the Pliocene Amazon Basin. Notably, a previous attempt to reconstruct paleotemperatures for the last deglaciation using brGDGTs in the Amazon River fan also resulted in a severe underestimation (~10 °C) of Holocene temperatures (Bendle et al., 2010), similar to the offset observed in our Pliocene record. Bendle et al. (2010) explained their underestimated temperatures

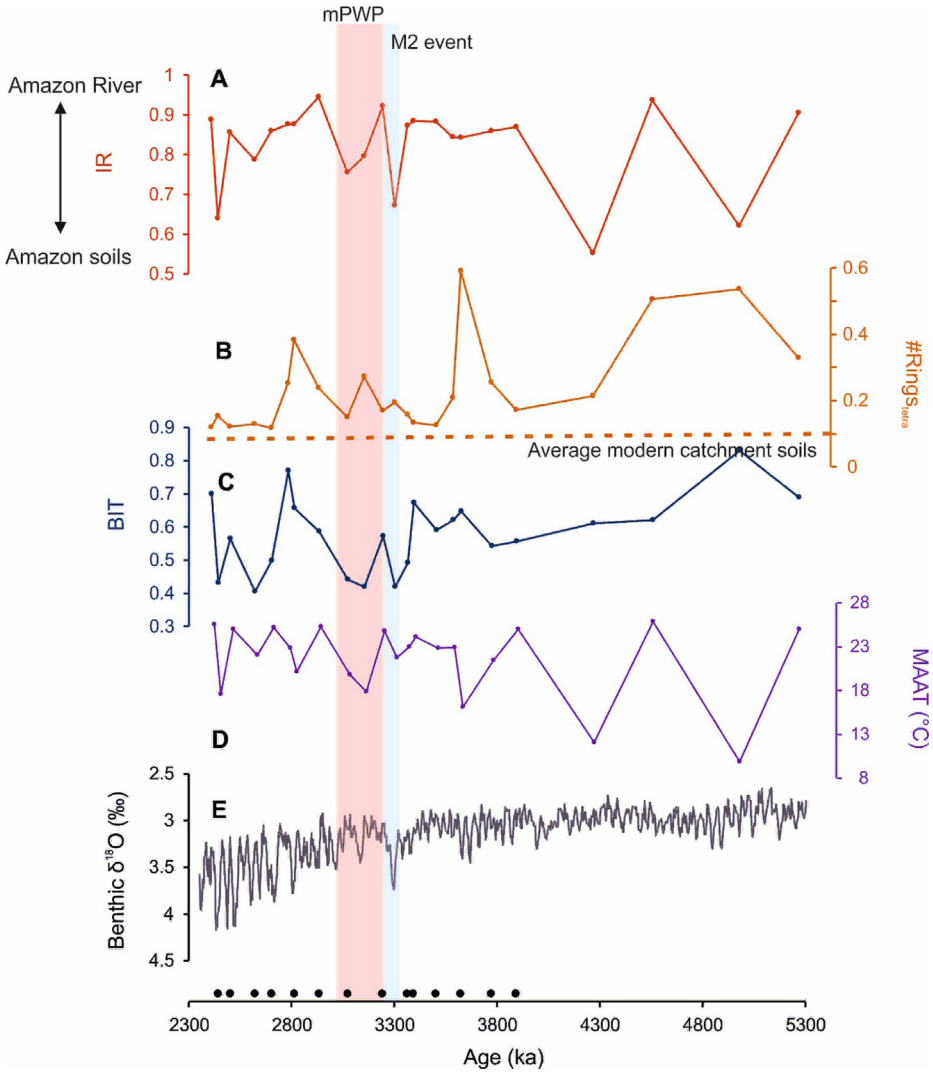

Fig. 5. Proxy records for the Pliocene ODP Site 925 sediments on the Ceará Rise: (A) IR, (B) #rings$_{tetra}$, (C) BIT, (D) MAAT, and (E) LR04 benthic $\delta^{18}O$ record plotted against age. Including 9 data points from van Soelen et al. (2017). Samples analysed for *n*-alkane composition (black circles) are shown on top of the age axis.

by an increased input of soil material from the high Andes, mobilized by melting glaciers. Although their brGDGT data were generated using the older HPLC method that does not separate 5- and 6-methyl isomers, our data suggest that a contribution of brGDGTs produced in the Amazon River may be responsible for their underestimated reconstructed temperatures instead. Where Zell et al. (2014) advised that brGDGT paleothermometry should only be applied to marine sediments under a heavy river influence, we suggest that even the river influence itself can overprint the soil signal and obscure the resulting reconstructed temperatures.

4. Conclusions

The generation of reliable Pliocene terrestrial air temperature records based on brGDGTs in marine sediments from the Gulf of Mexico (ODP Site 625) and the Ceará Rise (ODP Site 925) was hampered by contributions of brGDGTs from different sources overprinting the initial soil signal discharged by the Mississippi and Amazon Rivers, respectively. In the GoM, low BIT and high values of #rings$_{tetra}$ indicate that Site 625 did not receive sufficient terrestrial material, perhaps due to the different direction of the Mississippi River outflow during the Pliocene. The primarily marine source of the brGDGTs, coupled with near absence of pollen and leaf waxes, prohibited any correction method to remove the in situ brGDGT overprint and rendered these sediments unsuitable for brGDGT paleothermometry. Although the brGDGTs recovered from the Ceará Rise sediments have high BIT index and low #rings$_{tetra}$ values, implying a primarily soil-origin of the brGDGTs at this site, reconstructed MAATs underestimate the temperatures of the modern Amazon Basin by 8–20 °C, suggesting unrealistically low Pliocene temperatures for this area. We show that the large proportion of 6-methylated brGDGTS in the Ceará Rise sediments does not match the typical signature of modern soils from the Amazon watershed. Instead, the IR in the Ceará Rise sediments is closer to that of modern river SPM collected during the dry season, reflecting a contribution from riverine production. We postulate that a riverine contribution to the brGDGT pool in Amazon River fan sediments may have also complicated earlier attempts that used brGDGTs to generate temperature records for the Amazon Basin. This study shows that a mixed terrestrial/riverine/marine brGDGT source in marine sediments complicates the use of the soil-based brGDGT calibration in these settings. Therefore, future studies that aim to reconstruct temperature changes on the continent using these biomarkers should focus on establishing (i) terres-

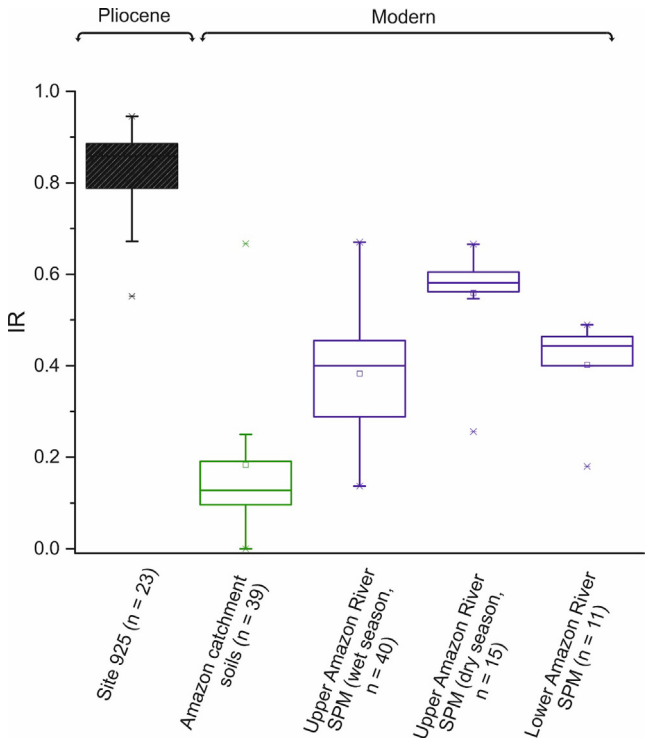

Fig. 6. Comparison of IR values across ODP Site 925 (Pliocene, this study and van Soelen et al., 2017), and modern Amazon River catchment soils (De Jonge et al., 2014a; Kirkels et al., 2020), Upper Amazon River SPM (wet and dry season; Kirkels et al., 2020), and Lower Amazon River SPM reanalysed from Zell et al. (2013a).

trial input in marine sediment sequences, and (ii) employing methods to disentangle relative contributions of brGDGT sources (cf. Dearing Crampton-Flood et al., 2018).

Declaration of Competing Interest

The authors declare that they have no known competing financial interests or personal relationships that could have appeared to influence the work reported in this paper.

Acknowledgements

The authors would like to acknowledge the Ocean Drilling Program Core repositories at Bremen and Texas A&M for providing access to core material. We thank David Naafs and Jonathan Raberg for constructive reviews that greatly improved the manuscript. We also thank Anita van Leeuwen (UU), Arnold van Dijk (UU), Martin Ziegler (UU), Cindy Schrader (UU), Marianne Baas (NIOZ), and Denise Dorhout (NIOZ) for analytical support. Stefan Schouten is thanked for providing feedback on an earlier version of this manuscript. This work was supported by funding from the Netherlands Earth System Science Center (NESSC) through a gravitation grant (NWO 024.002.001) from the Dutch Ministry for Education, Culture and Science.

Appendix A. Supplementary material

Supplementary data to this article can be found online at https://doi.org/10.1016/j.orggeochem.2021.104200.

Associate Editor—**Marcus Elvert**

References

Bendle, J.A., Weijers, J.W., Maslin, M.A., Sinninghe Damsté, J.S., Schouten, S., Hopmans, E.C., Boot, C.S., Pancost, R.D., 2010. Major changes in glacial and Holocene terrestrial temperatures and sources of organic carbon recorded in the Amazon fan by tetraether lipids. Geochemistry, Geophysics, Geosystems 11, Q12007.

Bentley Sr, S.J., Blum, M.D., Maloney, J., Pond, L., Paulsell, R., 2016. The Mississippi River source-to-sink system: Perspectives on tectonic, climatic, and anthropogenic influences, Miocene to Anthropocene. Earth-Science Reviews 153, 139–174.

Burke, K.D., Williams, J.W., Chandler, M.A., Haywood, A.M., Lunt, D.J., Otto-Bliesner, B.L., 2018. Pliocene and Eocene provide best analogs for near-future climates. Proceedings of the National Academy of Sciences 115, 13288–13293.

Ceccopieri, M., Carreira, R.S., Wagener, A.D.L.R., Hefter, J., Mollenhauer, G., 2019. Branched GDGTs as proxies in surface sediments from the south-eastern Brazilian continental margin. Frontiers in Earth Science 7, 291.

Coleman, J.M., 1988. Dynamic changes and processes in the Mississippi River delta. Geological Society of America Bulletin 100, 999–1015.

Curry, W.B., Shackleton, N.J., Richter, C., 1995. Leg 154. Synthesis. Proceedings of the Ocean Drilling Project, Initial Reports 154, 421–442.

de Boer, B., Haywood, A.M., Dolan, A.M., Hunter, S.J., Prescott, C.L., 2017. The transient response of ice volume to orbital forcing during the warm late Pliocene. Geophysical Research Letters 44, 486–494.

De Jonge, C., Hopmans, E.C., Stadnitskaia, A., Rijpstra, W.I.C., Hofland, R., Tegelaar, E., Sinninghe Damsté, J.S., 2013. Identification of novel penta- and hexamethylated branched glycerol dialkyl glycerol tetraethers in peat using HPLC–MS^2, GC–MS and GC–SMB-MS. Organic Geochemistry 54, 78–82.

De Jonge, C., Hopmans, E.C., Zell, C.I., Kim, J.H., Schouten, S., Sinninghe Damsté, J.S., 2014a. Occurrence and abundance of 6-methyl branched glycerol dialkyl glycerol tetraethers in soils: Implications for palaeoclimate reconstruction. Geochimica et Cosmochimica Acta 141, 97–112.

De Jonge, C., Stadnitskaia, A., Hopmans, E.C., Cherkashov, G., Fedotov, A., Sinninghe Damsté, J.S., 2014b. In situ produced branched glycerol dialkyl glycerol tetraethers in suspended particulate matter from the Yenisei River, Eastern Siberia. Geochimica et Cosmochimica Acta 125, 476–491.

De Jonge, C., Stadnitskaia, A., Hopmans, E.C., Cherkashov, G., Fedotov, A., Streletskaya, I.D., Vasiliev, A.A., Sinninghe Damsté, J.S., 2015. Drastic changes in the distribution of branched tetraether lipids in suspended matter and sediments from the Yenisei River and Kara Sea (Siberia): Implications for the use of brGDGT-based proxies in coastal marine sediments. Geochimica et Cosmochimica Acta 165, 200–225.

Dearing Crampton-Flood, E., Peterse, F., Munsterman, D., Sinninghe Damsté, J.S., 2018. Using tetraether lipids archived in North Sea Basin sediments to extract North Western European Pliocene continental air temperatures. Earth and Planetary Science Letters 490, 193–205.

Dearing Crampton-Flood, E., Tierney, J.E., Peterse, F., Kirkels, F.M., Sinninghe Damsté, J.S., 2020. BayMBT: A Bayesian calibration model for branched glycerol dialkyl glycerol tetraethers in soils and peats. Geochimica et Cosmochimica Acta 268, 142–159.

Ding, S., Xu, Y., Wang, Y., He, Y., Hou, J., Chen, L., He, J.S., 2015. Distribution of branched glycerol dialkyl glycerol tetraethers in surface soils of the Qinghai-Tibetan Plateau: implications of brGDGTs-based proxies in cold and dry regions. Biogeosciences 12, 3141–3151.

Elsik, W.C., 1969. Late Neogene palynomorph diagram, northern Gulf of Mexico. Gulf Coast Association of Geological Societies Transactions 19, 509–528.

Figueiredo, J.J.J.P., Hoorn, C., Van der Ven, P., Soares, E., 2009. Late Miocene onset of the Amazon River and the Amazon deep-sea fan: Evidence from the Foz do Amazonas Basin. Geology 37, 619–622.

Freymond, C.V., Peterse, F., Fischer, L.V., Filip, F., Giosan, L., Eglinton, T.I., 2017. Branched GDGT signals in fluvial sediments of the Danube River basin: Method comparison and longitudinal evolution. Organic Geochemistry 103, 88–96.

Galloway, W.E., Whiteaker, T.L., Ganey-Curry, P., 2011. History of Cenozoic North American drainage basin evolution, sediment yield, and accumulation in the Gulf of Mexico basin. Geosphere 7, 938–973.

Grant, G.R., Naish, T.R., Dunbar, G.B., Stocchi, P., Kominz, M.A., Kamp, P.J., Tapia, C.A., McKay, R.M., Levy, R.H., Patterson, M.O., 2019. The amplitude and origin of sea-level variability during the Pliocene epoch. Nature 574, 237–241.

Guo, J., Glendell, M., Meersmans, J., Kirkels, F., Middelburg, J.J., Peterse, F., 2020. Assessing branched tetraether lipids as tracers of soil organic carbon transport through the Carminowe Creek catchment (southwest England). Biogeosciences 17, 3183–3201.

Harris, I.P.D.J., Jones, P.D., Osborn, T.J., Lister, D.H., 2014. Updated high-resolution grids of monthly climatic observations–the CRU TS3. 10 Dataset. International Journal of Climatology 34, 623–642.

Harvey, H.R., Fallon, R.D., Patton, J.S., 1986. The effect of organic matter and oxygen on the degradation of bacterial membrane lipids in marine sediments. Geochimica et Cosmochimica Acta 50, 795–804.

Haywood, A.M., Dowsett, H.J., Dolan, A.M., 2016. Integrating geological archives and climate models for the mid-Pliocene warm period. Nature Communications 7, 10646.

Haywood, A.M., Tindall, J.C., Dowsett, H.J., Dolan, A.M., Foley, K.M., Hunter, S.J., Hill, D.J., Chan, W.L., Abe-Ouchi, A., Stepanek, C., Lohmann, G., Chandan, D., Peltier, W.R., Tan, N., Contoux, C., Ramstein, G., Li, X., Zhang, Z., Guo, C., Nisancioglu, K. H., Zhang, Q., Li, Q., Kamae, Y., Chandler, M.A., Sohl, L.E., Otto-Bliesner, B.L., Feng,

R., Brady, E.C., von der Heydt, A.S., Baatsen, M.L.J., Lunt, D.J., 2020. The Pliocene Model Intercomparison Project Phase 2: large-scale climate features and climate sensitivity. Climate of the Past Discussions 16, 2095–2123.
Herbert, T.D., Peterson, L.C., Lawrence, K.T., Liu, Z., 2010. Tropical ocean temperatures over the past 3.5 million years. Science 328, 1530–1534.
Hopmans, E.C., Weijers, J.W., Schefuß, E., Herfort, L., Sinninghe Damsté, J.S., Schouten, S., 2004. A novel proxy for terrestrial organic matter in sediments based on branched and isoprenoid tetraether lipids. Earth and Planetary Science Letters 224, 107–116.
Hopmans, E.C., Schouten, S., Sinninghe Damsté, J.S., 2016. The effect of improved chromatography on GDGT-based palaeoproxies. Organic Geochemistry 93, 1–6.
Huguet, C., Hopmans, E.C., Febo-Ayala, W., Thompson, D.H., Sinninghe Damsté, J.S., Schouten, S., 2006. An improved method to determine the absolute abundance of glycerol dibiphytanyl glycerol tetraether lipids. Organic Geochemistry 37, 1036–1041.
Joyce, J.E., Tjalsma, L.R., Prutzman, J.M., 1990. High-resolution planktic stable isotope record and spectral analysis for the last 5.35 MY: Ocean Drilling Program Site 625 northeast Gulf of Mexico. Paleoceanography 5, 507–529.
Kemp, D.B., Robinson, S.A., Crame, J.A., Francis, J.E., Ineson, J., Whittle, R.J., Bowman, V., O'Brien, C., 2014. A cool temperate climate on the Antarctic Peninsula through the latest Cretaceous to early Paleogene. Geology 42, 583–586.
Kim, J.H., Zell, C., Moreira-Turcq, P., Pérez, M.A., Abril, G., Mortillaro, J.M., Weijers, J. W., Meziane, T., Sinninghe Damsté, J.S., 2012. Tracing soil organic carbon in the lower Amazon River and its tributaries using GDGT distributions and bulk organic matter properties. Geochimica et Cosmochimica Acta 90, 163–180.
Kirkels, F.M., Ponton, C., Galy, V., West, A.J., Feakins, S.J., Peterse, F., 2020. From Andes to Amazon: assessing branched tetraether lipids as tracers for soil organic carbon in the Madre de Dios River system. Journal of Geophysical Research: Biogeosciences 125, e2019JG005270.
Lammertsma, E.I., Troelstra, S.R., Flores, J.A., Sangiorgi, F., Chemale, F., do Carmo, D. A., Hoorn, C., 2018. Primary productivity in the western tropical Atlantic follows Neogene Amazon River evolution. Palaeogeography, Palaeoclimatology, Palaeoecology 506, 12–21.
Li, Z., Peterse, F., Wu, Y., Bao, H., Eglinton, T.I., Zhang, J., 2015. Sources of organic matter in Changjiang (Yangtze River) bed sediments: preliminary insights from organic geochemical proxies. Organic Geochemistry 85, 11–21.
Limoges, A., de Vernal, A., Van Nieuwenhove, N., 2014. Long-term hydrological changes in the northeastern Gulf of Mexico (ODP-625B) during the Holocene and late Pleistocene inferred from organic-walled dinoflagellate cysts. Palaeogeography, Palaeoclimatology, Palaeoecology 414, 178–191.
Lisiecki, L.E., Raymo, M.E., 2005. A Pliocene-Pleistocene stack of 57 globally distributed benthic $\delta^{18}O$ records. Paleoceanography 20, PA1003.
Martinez, J.M., Guyot, J.L., Filizola, N., Sondag, F., 2009. Increase in suspended sediment discharge of the Amazon River assessed by monitoring network and satellite data. Catena 79, 257–264.
Masson-Delmotte, V., Schulz, M., Abe-Ouchi, A., 2013. Information from paleoclimate archives. In: Stocker, T.F., Qin, D., Plattner, G.-K. (Eds.), Climate Change 2013: The Physical Science Basis. Contribution of Working Group I to the Fifth Assessment Report of the Intergovernmental Panel on Climate Change. Cambridge University Press, Cambridge and New York, pp. 383–464.
Moreira, A., Fageria, N.K., 2009. Soil chemical attributes of Amazonas state, Brazil. Communications in Soil Science and Plant Analysis 40, 2912–2925.
Moreira, L.S., Moreira-Turcq, P., Kim, J.H., Turcq, B., Cordeiro, R.C., Caquineau, S., Mandengo-Yogo, M., Sinninghe Damsté, J.S., 2014. A mineralogical and organic geochemical overview of the effects of Holocene changes in Amazon River flow on three floodplain lakes. Palaeogeography, Palaeoclimatology, Palaeoecology 415, 152–164.
Naafs, B.D.A., Gallego-Sala, A.V., Inglis, G.N., Pancost, R.D., 2017. Refining the global branched glycerol dialkyl glycerol tetraether (brGDGT) soil temperature calibration. Organic Geochemistry 106, 48–56.
Nürnberg, D., Ziegler, M., Karas, C., Tiedemann, R., Schmidt, M.W., 2008. Interacting Loop Current variability and Mississippi River discharge over the past 400 kyr. Earth and Planetary Science Letters 272, 278–289.
Peterse, F., Kim, J.H., Schouten, S., Kristensen, D.K., Koç, N., Sinninghe Damsté, J.S., 2009. Constraints on the application of the MBT/CBT palaeothermometer at high latitude environments (Svalbard, Norway). Organic Geochemistry 40, 692–699.
Pound, M.J., Tindall, J., Pickering, S.J., Haywood, A.M., Dowsett, H.J., Salzmann, U., 2014. Late Pliocene lakes and soils: a global data set for the analysis of climate feedbacks in a warmer world. Climate of the Past 10, 167–180.
Rabinowitz, P.D., Merrell, W.J., Garrison, L.E., Kidd, R.B., Garrison, E., 1985. Ocean Drilling Program Leg 100 Report Northeastern Gulf of Mexico.
Sangiorgi, F., Bijl, P.K., Passchier, S., Salzmann, U., Schouten, S., McKay, R., Cody, R.D., Pross, J., Van De Flierdt, T., Bohaty, S.M., Levy, R., 2018. Southern Ocean warming and Wilkes Land ice sheet retreat during the mid-Miocene. Nature Communications 9, 1–11.
Schouten, S., Hopmans, E.C., Sinninghe Damsté, J.S., 2013. The organic geochemistry of glycerol dialkyl glycerol tetraether lipids: a review. Organic Geochemistry 54, 19–61.
Shackleton, N.J., 1974. Attainment of isotopic equilibrium between ocean water and the benthonic foraminifera genus Uvigerina: isotopic changes in the ocean during the last glacial. Les methods quantitatives d'étude de variations du climat au cours du Pleistocène, Gif-sur-Yvette. Colloque international du CNRS 219, 203–210.
Shakun, J.D., Raymo, M.E., Lea, D.W., 2016. An early Pleistocene Mg/Ca-$\delta^{18}O$ record from the Gulf of Mexico: evaluating ice sheet size and pacing in the 41-kyr world. Paleoceanography 31, 1011–1027.
Sinninghe Damsté, J.S., 2016. Spatial heterogeneity of sources of branched tetraethers in shelf systems: the geochemistry of tetraethers in the Berau River delta (Kalimantan, Indonesia). Geochimica et Cosmochimica Acta 186, 13–31.
Sinninghe Damsté, J.S., Hopmans, E.C., Pancost, R.D., Schouten, S., Geenevasen, J.A., 2000. Newly discovered non-isoprenoid glycerol dialkyl glycerol tetraether lipids in sediments. Chemical Communications 17, 1683–1684.
Sinninghe Damsté, J.S., Schouten, S., Hopmans, E.C., van Duin, A.C., Geenevasen, J.A., 2002. Crenarchaeol the characteristic core glycerol dibiphytanyl glycerol tetraether membrane lipid of cosmopolitan pelagic crenarchaeota. Journal of Lipid Research 43, 1641–1651.
Sinninghe Damsté, J.S., Rijpstra, W.I.C., Hopmans, E.C., Weijers, J.W., Foesel, B.U., Overmann, J., Dedysh, S.N., 2011. 13,16-Dimethyl octacosanedioic acid (iso-diabolic acid), a common membrane-spanning lipid of Acidobacteria subdivisions 1 and 3. Applied and Environmental Microbiology 77, 4147–4154.
Sinninghe Damsté, J.S., Rijpstra, W.I.C., Foesel, B.U., Huber, K.J., Overmann, J., Nakagawa, S., Kim, J.J., Dunfield, P.F., Dedysh, S.N., Villanueva, L., 2018. An overview of the occurrence of ether- and ester-linked iso-diabolic acid membrane lipids in microbial cultures of the Acidobacteria: Implications for brGDGT paleoproxies for temperature and pH. Organic Geochemistry 124, 63–67.
Sparkes, R.B., Doğrul Selver, A., Bischoff, J., Talbot, H.M., Gustafsson, Ö., Semiletov, I. P., Dudarev, O.V., van Dongen, B.E., 2015. GDGT distributions on the East Siberian Arctic Shelf: implications for organic carbon export, burial and degradation. Biogeosciences 12, 3753–3768.
Super, J.R., Chin, K., Pagani, M., Li, H., Tabor, C., Harwood, D.M., Hull, P.M., 2018. Late Cretaceous climate in the Canadian Arctic: multi-proxy constraints from Devon Island. Palaeogeography, Palaeoclimatology, Palaeoecology 504, 1–22.
Tipple, B.J., Pagani, M., 2010. A 35Myr North American leaf-wax compound-specific carbon and hydrogen isotope record: implications for C4 grasslands and hydrologic cycle dynamics. Earth and Planetary Science Letters 299, 250–262.
Tripsanas, E.K., Bryant, W.R., Slowey, N.C., Bouma, A.H., Karageorgis, A.P., Berti, D., 2007. Sedimentological history of Bryant Canyon area, northwest Gulf of Mexico, during the last 135 kyr (Marine Isotope Stages 1–6): a proxy record of Mississippi River discharge. Palaeogeography, Palaeoclimatology, Palaeoecology 246, 137–161.
van Soelen, E.E., Kim, J.H., Santos, R.V., Dantas, E.L., de Almeida, F.V., Pires, J.P., Roddaz, M., Sinninghe Damsté, J.S., 2017. A 30 Ma history of the Amazon River inferred from terrigenous sediments and organic matter on the Ceará Rise. Earth and Planetary Science Letters 474, 40–48.
Warden, L., Kim, J.H., Zell, C., Vis, G.J., Stigter, H.D., Bonnin, J., Sinninghe Damsté, J.S., 2016. Examining the provenance of branched GDGTs in the Tagus River drainage basin and its outflow into the Atlantic Ocean over the Holocene to determine their usefulness for paleoclimate applications. Biogeosciences 13, 5719–5738.
Warden, L., Moros, M., Weber, Y., Sinninghe Damsté, J.S., 2018. Change in provenance of branched glycerol dialkyl glycerol tetraethers over the Holocene in the Baltic Sea and its impact on continental climate reconstruction. Organic Geochemistry 121, 138–154.
Weijers, J.W., Schouten, S., Hopmans, E.C., Geenevasen, J.A., David, O.R., Coleman, J. M., Pancost, R.D., Sinninghe Damsté, J.S., 2006. Membrane lipids of mesophilic anaerobic bacteria thriving in peats have typical archaeal traits. Environmental Microbiology 8, 648–657.
Weijers, J.W., Schouten, S., van den Donker, J.C., Hopmans, E.C., Sinninghe Damsté, J. S., 2007a. Environmental controls on bacterial tetraether membrane lipid distribution in soils. Geochimica et Cosmochimica Acta 71, 703–713.
Weijers, J.W., Schefuß, E., Schouten, S., Sinninghe Damsté, J.S., 2007b. Coupled thermal and hydrological evolution of tropical Africa over the last deglaciation. Science 315, 1701–1704.
Weijers, J.W., Schouten, S., Sluijs, A., Brinkhuis, H., Sinninghe Damsté, J.S., 2007c. Warm arctic continents during the Palaeocene-Eocene thermal maximum. Earth and Planetary Science Letters 261, 230–238.
Weijers, J.W., Panoto, E., van Bleijswijk, J., Schouten, S., Rijpstra, W.I.C., Balk, M., Stams, A.J., Sinninghe Damsté, J.S., 2009. Constraints on the biological source(s) of the orphan branched tetraether membrane lipids. Geomicrobiology Journal 26, 402–414.
Weijers, J.W.H., Wiesenberg, G.L., Bol, R., Hopmans, E.C., Pancost, R.D., 2010. Carbon isotopic composition of branched tetraether membrane lipids in soils suggest a rapid turnover and a heterotrophic life style of their source organism(s). Biogeosciences 7, 2959–2973.
White, D.C., Davis, W.M., Nickels, J.S., King, J.D., Bobbie, R.J., 1979. Determination of the sedimentary microbial biomass by extractible lipid phosphate. Oecologia 40, 51–62.
Wilkens, R., Westerhold, T., Drury, A.J., Lyle, M., Gorgas, T., Tian, J., 2017. Revisiting the Ceara Rise, equatorial Atlantic Ocean: isotope stratigraphy of ODP Leg 154. Climate of the Past 13, 779–793.
Woodbury, H.O., Murray Jr, I.B., Pickford, P.J., Akers, W.H., 1974. Pliocene and Pleistocene depocenters, outer continental shelf, Louisiana and Texas. American Association of Petroleum Geologists Bulletin 57, 2428–2439.
Xiao, W., Wang, Y., Liu, Y., Zhang, X., Shi, L., Xu, Y., 2020. Predominance of hexamethylated 6-methyl branched glycerol dialkyl glycerol tetraethers in the Mariana Trench: source and environmental implication. Biogeosciences 17, 2135–2148.

Xu, Y., Jia, Z., Xiao, W., Fang, J., Wang, Y., Luo, M., Wenzhöfer, F., Rowden, A.A., Glud, R.N., 2020. Glycerol dialkyl glycerol tetraethers in surface sediments from three Pacific trenches: Distribution, source and environmental implications. Organic Geochemistry 147, 104079.

Yang, G., Zhang, C.L., Xie, S., Chen, Z., Gao, M., Ge, Z., Yang, Z., 2013. Microbial glycerol dialkyl glycerol tetraethers from river water and soil near the Three Gorges Dam on the Yangtze River. Organic Geochemistry 56, 40–50.

Yang, H., Lü, X., Ding, W., Lei, Y., Dang, X., Xie, S., 2015. The 6-methyl branched tetraethers significantly affect the performance of the methylation index (MBT′) in soils from an altitudinal transect at Mount Shennongjia. Organic Geochemistry 82, 42–53.

Zell, C., Kim, J.H., Moreira-Turcq, P., Abril, G., Hopmans, E.C., Bonnet, M.P., Sobrinho, R.L., Sinninghe Damsté, J.S., 2013a. Disentangling the origins of branched tetraether lipids and crenarchaeol in the lower Amazon River: implications for GDGT-based proxies. Limnology and Oceanography 58, 343–353.

Zell, C., Kim, J.H., Abril, G., Sobrinho, R., Dorhout, D., Moreira-Turcq, P., Sinninghe Damsté, J., 2013b. Impact of seasonal hydrological variation on the distributions of tetraether lipids along the Amazon River in the central Amazon basin: implications for the MBT/CBT paleothermometer and the BIT index. Frontiers in Microbiology 4, 228.

Zell, C., Kim, J.H., Hollander, D., Lorenzoni, L., Baker, P., Silva, C.G., Nittrouer, C., Sinninghe Damsté, J.S., 2014. Sources and distributions of branched and isoprenoid tetraether lipids on the Amazon shelf and fan: Implications for the use of GDGT-based proxies in marine sediments. Geochimica et Cosmochimica Acta 139, 293–312.

Zell, C., Kim, J.H., Dorhout, D., Baas, M., Sinninghe Damsté, J.S., 2015. Sources and distributions of branched tetraether lipids and crenarchaeol along the Portuguese continental margin: Implications for the BIT index. Continental Shelf Research 96, 34–44.

Zhang, C., Wang, J., Wei, Y., Zhu, C., Huang, L., Dong, H., 2012. Production of branched tetraether lipids in the lower Pearl River and estuary: effects of extraction methods and impact on bGDGT proxies. Frontiers in Microbiology 2, 274.

Zhu, C., Weijers, J.W., Wagner, T., Pan, J.M., Chen, J.F., Pancost, R.D., 2011. Sources and distributions of tetraether lipids in surface sediments across a large river-dominated continental margin. Organic Geochemistry 42, 376–386.